ternatively, it may be of interest to employ the final energy distributions of the fragments computed here in studies addressing the classical reaction dynamics of the $CH_2N_2O_2$ system.

We make a final comment concerning the applicability of the classical trajectory method to full-dimensional studies of the intramolecular reaction dynamics in large polyatomic systems. Using a relatively simple form for the potential energy surface that incorporates attenuation of the intramolecular forces in a straightforward (if somewhat cumbersome) manner, we have been able to reproduce the available experimental data with reasonably good accuracy. This is in spite of almost complete lack of knowledge of the details of the potential energy surface in regions other than those corresponding to the reactants and products. This suggests that it may be possible to extend the scope of these kinds of studies to other large chemical systems.

Note Added in Proof. After this work was completed, an experimental gas-phase structure for RDX was reported [Shishkov, I. F.; Vilkov, L. V.; Kolonits, M.; Rozsondai, B. *Struct. Chem.* **1991**, *2*, 57]. Our assumed structure is in good agreement with the measured structure.

Acknowledgment. We thank Drs. Page and Adams (ref 25) for making some of their data available to us prior to publication. We are grateful to Dr. B. M. Rice for invaluable comments concerning the calculations. We also acknowledge a grant of computer time on the IBM 3090-200S computer at Oklahoma State University. Some of the calculations reported here were carried out using the CRAY X-MP/48 at the U.S. Army Ballistics Research Laboratories. This work was supported by the U.S. Army Research Office.

Bleaching of the Bacteriochlorophyll Monomer Band: Can Absorption Kinetics Distinguish Virtual from Two-Step Electron Transfer in Bacterial Photosynthesis?

Julian S. Joseph,*,† William Bruno,‡,∥ and William Bialek‡,§,⊥

Graduate Group in Biophysics, Department of Physics, and Department of Molecular and Cell Biology, University of California at Berkeley, Berkeley, California 94720, and NEC Research Institute, 4 Independence Way, Princeton, New Jersey 08540 *(Received: September 21, 1990; In Final Form: March 7, 1991)*

The significance of absorption kinetics data in distinguishing between two-step and virtual mechanisms for the primary charge separation in reaction centers of photosynthetic bacteria is examined. A simple class of models is presented in which the transfer may occur predominantly by a virtual process and in which the intermediate state develops some small, but nonzero, transient population. The simplicity of the model allows both the virtual and two-step contributions to the intermediate state population to be easily calculated. We find that the peak intermediate state population can be either close to 1 or very small ($<10^{-2}$), depending on the system parameters such as electronic matrix elements, the energy denominator, and the lifetimes and dephasing rates in the electronic states. In particular, purely virtual transfer can yield a peak intermediate-state population of 10%. These calculations imply that observation of a small amount of bleaching in the bacteriochlorophyll monomer band does not necessarily rule out a virtual process.

Introduction

One of the outstanding questions in the study of bacterial photosynthesis is the mechanism of the primary charge separation from the excited special pair to the bacteriopheophytin ($P^*H \rightarrow P^+H^-$). In the hope of elucidating this mechanism, there has been a considerable amount of experimental interest[1-7] in detecting bleaching of the bacteriochlorophyll monomer (B) absorption band in purple photosynthetic bacteria. The two most commonly discussed transfer mechanisms are a sequential two-step process[8,9] and a virtual transition[10-12] (often termed "superexchange") through the state P^+B^-. A third possibility in which, like perturbative virtual transfer, coherence is maintained in the intermediate has also been explored recently.[13,14]

It is usually assumed that observation of population in the state B^- (depletion of the state B) is an unambiguous signature of the two-step process. In the original experiments of Martin et al.,[1] probing with 150-fs pulses showed no such bleaching of the absorption band associated with the state B. Holzapfel and coworkers[5,6] reported measurements of the absorption kinetics that are purported to indicate a depletion of the neutral unexcited monomer population by as much as 15%. It is then asserted that their data implies a two-step mechanism for the primary transfer. Kirmaier and Holten,[7] however, recently reported a failure to resolve any signature of the state P^+B^- in the absorption kinetics under essentially the same experimental conditions. It is asserted in ref 15 that virtual transfer implies no transient population on the intermediate state. Our main objective in this paper is to point out that even in the virtual transfer process there should be some

† Graduate Group in Biophysics. Current address: Laboratory of Sensorimotor Research, National Eye Institute, NIH, Bethesda, MD 20892.
‡ Department of Physics.
§ Department of Molecular and Cell Biology.
⊥ NEC Research Institute.
∥ Current address: Center for Nonlinear Studies, Los Alamos National Laboratory, Los Alamos, NM 87545.

(1) Martin, J.-L.; Breton, J.; Hoff, A. J.; Migus, A.; Antonetti, A. *Proc. Natl. Acad. Sci. U.S.A.* **1986**, *83*, 957.
(2) Breton, J.; Martin, J.-L.; Petrich, J.; Migus, A.; Antonetti, A. *FEBS Lett.* **1986**, *209*, 37.
(3) Breton, J.; Martin, J.-L.; Migus, A.; Antonetti, A.; Orszag, A. *Proc. Natl. Acad. Sci. U.S.A.* **1986**, *83*, 5121.
(4) Martin, J.-L.; Breton, J.; Lambry, J. C.; Fleming, G. In *The Photosynthetic Bacterial Reaction Center: Structure and Dynamics. NATO ASI Series*; Breton, J., Vermeglio, A., Eds.; Plenum Press: New York, 1987.
(5) Holzapfel, W.; Finkele, U.; Kaiser, W.; Oesterhelt, D.; Scheer, H.; Stilz, H. U.; Zinth, W. *Chem. Phys. Lett.* **1989**, *160*, 1.
(6) Holzapfel, W.; Finkele, U.; Kaiser, W.; Oesterhelt, D.; Scheer, H.; Stilz, H. U.; Zinth, W. *Proc. Natl. Acad. Sci. U.S.A.* **1990**, *87*, 5168.
(7) Kirmaier, C.; Holten, D. *Biochemistry* **1991**, *30*, 609.
(8) Creighton, S.; Hwang, J.-K.; Warshel, A. *Biochemistry* **1988**, *27*, 774.
(9) Marcus, R. A. *Chem. Phys. Lett.* **1987**, *133*, 471.
(10) Lockhart, D. J.; Golstein, R. F.; Boxer, S. G. *J. Chem. Phys.* **1988**, *89*, 1408.
(11) Bixon, M.; Jortner, J. *J. Phys. Chem.* **1988**, *92*, 7148.
(12) Kuznetsov, A. M.; Ulstrup, J.; Zakaraya, M. G. In *Perspectives in Photosynthesis*; Jortner, J., Pullman, B., Eds.; D. Reidel Publishing Co.: Dordrecht, Holland, 1990.
(13) Marcus, R. A.; Almeida, R. *J. Phys. Chem.* **1990**, *94*, 2973.
(14) Almeida, R.; Marcus, R. A. *J. Phys. Chem.* **1990**, *94*, 2978.
(15) Hu, Y.; Mukamel, S. *Chem. Phys. Lett.* **1989**, *160*, 410.

0022-3654/91/2095-6242$02.50/0

bleaching in the B band, although it may be small. Therefore, the observation of some bleaching does not rule out a virtual transfer process for the primary charge separation.

By virtual transfer we mean a transition through an intermediate state such that the phase of the state vector is not significantly randomized in the intermediate state. The transition to the intermediate may or may not conserve energy. In a two-step process, the phase is completely randomized (i.e., phase coherence is completely destroyed) in the intermediate state, and the intermediate state is said to be a real or chemical intermediate. This allows the existence of a well-defined rate for transfer from the initial to the intermediate electronic state, in contrast to virtual transfer in which there is no such rate. Note that while probing with a laser pulse to measure the population in the intermediate state does interrupt the coherent evolution of the electronic state, it is a correct measurement of the population in the intermediate state at the time the probe arrives, provided that the experiment is started over with a new excitation before probing again.

Virtual transfer allows single-exponential growth of the final-state population even though there is no direct coupling between initial and final states. During any reaction proceeding by a virtual process, there is however some amplitude on the virtual intermediate state,[16] although this amplitude may be small. The presence of nonzero amplitude on the virtual intermediate directly implies a nonzero population for that state. In the case of the primary charge transfer, this in turn implies a nonzero bleaching of the monomer band. The precise magnitude of this bleaching varies widely as certain parameters of the system, such as electronic matrix elements and dephasing rates, are varied from one regime into another. We discuss in various scenarios how large the intermediate state population can become and how it varies with time. In the extreme case of absolutely no dephasing in the intermediate state, we will see that the intermediate state population can approach 1, which, although clearly contradictory to experiment, emphasizes the fact that the intermediate state population can become sizable even in a purely virtual transfer process.

It is not our intention here to propose any particular scheme for the primary charge separation. Indeed, there are many issues surrounding the primary charge separation that we do not address, for instance, the question of why the rate is so fast. However, the regimes we investigate are motivated by the need to understand the rapidity of the transfer. In particular, a regime with low but nonvanishing dephasing rates is seen to yield a fast reaction occurring largely by virtual transfer accompanied by a significant transient intermediate state population.

Simple Model

First consider a very simple system consisting of only two states separated by an energy E and coupled by a matrix element $V_{12} \ll E$. If we place the system in state 1 at time $t = 0$, amplitude on state 2 oscillates at the frequency $E/\hbar$, where $\hbar$ is Planck's constant divided by 2π. The maximum amplitude attained on state 2 has a magnitude $2V_{12}/E$. This is related to the fact that one of the energy eigenstates of the system is state 1 with an admixture $-V_{12}/E$ of state 2. This process of coherent mixing between states is essential to any virtual process. State 2 here crudely represents a virtual intermediate from state 1 to some third state that has not yet been considered.

To investigate more fully the population of the virtual intermediate state in various regimes of interest, we consider a three-state model that is still highly simplified and that exhibits virtual transfer. The model is illustrated in Figure 1a. We have in mind a simplified representation of three electronic states each of which possesses a set of vibrational levels; the three states in our simple model represent one vibrational level from each of the three electronic states P^*BH, P^+B^-H, and P^+BH^-. [This simplified representation of the more complicated problem of three vibrational surfaces is meaningful when the modes most strongly coupled to the electronic transitions are underdamped and when the transitions are nonadiabatic (the Landau–Zener transition probabilities are small). For clarity, we restrict ourselves here to these situations, although simplified representations might be useful in other cases as well.] If the intermediate state is PB^+H^- or PB^*H instead of P^+B^-H, everything we will say about the model will still be true. The system starts in state 1 at time $t = 0$; state 3 is degenerate with state 1, while state 2 is situated above state 1 by an energy E. Matrix elements V_{12} and V_{23} couple states 1 with 2 and states 2 with 3, respectively. Amplitude is depleted from state 3 at a rate Γ to ensure the existence of a well-defined rate constant from state 1 to state 3; equivalently, one could replace state 3 by a density of states $\rho_3 = 1/(\hbar\Gamma)$ as long as $\hbar\Gamma \gg V$, where V typifies the magnitudes of V_{12} and V_{23}. The time evolution of the amplitudes of the three states is described by the 3×3 (non-Hermitian) Hamiltonian

$$H = \begin{pmatrix} 0 & V_{12} & 0 \\ V_{12} & E & V_{23} \\ 0 & V_{23} & -i\hbar\Gamma \end{pmatrix} \tag{1}$$

This model provides an example of a system exhibiting virtual transfer in which the population of the virtual intermediate state can be easily calculated. If we assume $V_{12}, V_{23} \ll E \ll \hbar\Gamma$, the population of state 2 at time t after excitation can be approximated as

$$P_2(t) \simeq \left(\frac{V_{12}}{E}\right)^2 \left| \exp\left\{ i\frac{V_{12}^2}{E} t/\hbar - \left(\frac{V_{12}V_{23}}{E}\right)^2 \frac{1}{\hbar\Gamma} t/\hbar \right\} - \exp\left\{ -iEt/\hbar - \frac{V_{23}^2}{\hbar\Gamma} t/\hbar \right\} \right|^2 \tag{2}$$

The decay rate $(V_{12}V_{23}/E)^2/(\hbar^2\Gamma)$ corresponds to the virtual rate constant and in this case is the rate at which the total amplitude decays. The $V_{12}^2/(\hbar E)$ oscillation frequency of the first term simply represents a small energy shift due to the coupling between states 1 and 2. The second term is essentially a transient that decays away at the (fast) rate $k_{23} = 2V_{23}^2/(\hbar^2\Gamma)$. If instead $V_{12}, V_{23} \ll \hbar\Gamma \ll E$, the expression is the same except the transient decay rate is replaced by $k_{23} = 2V_{23}^2\Gamma/E^2$. Either way, the virtual rate constant can be identified as

$$k_{13} \simeq 2\left(\frac{V_{12}V_{23}}{E}\right)^2 \frac{1}{\hbar^2\Gamma} \tag{3}$$

The population of the final electronic state grows as a single exponential described by this rate constant, except at very short times less than $1/k_{23}$. By comparison, the state 2 population rises very quickly in a time $\sim\hbar/E$ and decays with the two time constants k_{23} and k_{13}. From eq 2 it can be seen that the maximum state 2 population is

$$P_{2MAX} \sim 4(V_{12}/E)^2 \tag{4}$$

which by hypothesis is small compared to 1. Here we have a system in which all the transfer happens by passing coherently through the intermediate state, i.e., virtual transfer, and yet there is some nonzero, although small, population on the intermediate during the course of the reaction. [There are a few features of this model that should not be taken too seriously, due to the highly simplified nature of the model. For example, at very short times, there are rapid oscillations at the frequency $E/\hbar$. It should be emphasized that these oscillations may not be observable in the real system, because the system has many different vibrational levels, each of which is broadened by damping and other dephasing processes and by inhomogeneous broadening.]

One might imagine that to ensure fast charge separation, the reaction center has engineered a small value of E. Naively, this means that $P_{2MAX} \sim 4(V_{12}/E)^2$ can become large. In fact with $E \sim (6\text{–}7)V_{12}$ (which still qualifies as $E \gg V_{12}$) $P_{2MAX} \sim 0.1$, which is not small. Intermediate state populations of order 5–10% might thus be consistent with purely virtual transfer even in the simple "perturbative" limit $V \ll E$. This result by itself is sufficient

(16) Sakaurai, J. J. *Modern Quantum Mechanics*; Benjamin/Cummings: Menlo Park, CA, 1985; p 333.

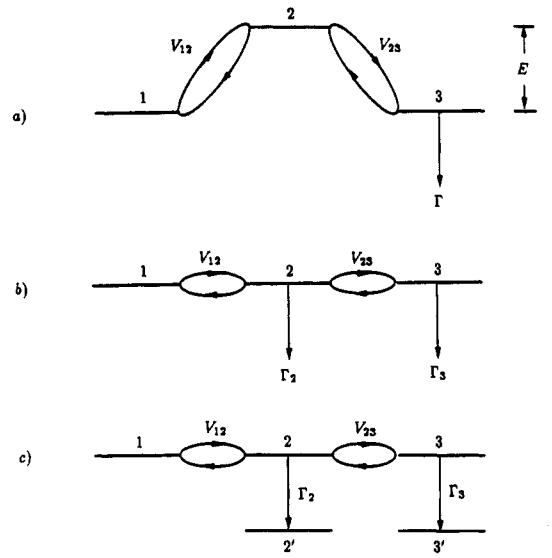

Figure 1. (a) Simple three-state model. States 1 and 3 are degenerate, while state 2 is separated by an energy E. The states mix via the couplings V_{12} and V_{23}. State 3 decays at a rate Γ. These states symbolize vibrational levels of three electronic states participating in the primary transfer. (b) Model modified by the addition of decay in state 2. The energy denominator E has been set to 0 to help get a fast rate. (c) The inclusion of additional states 2' and 3', which represent the other vibrational levels of electronic states 2 and 3. This is a convenient device for estimating the total population observed on the electronic states.

to show that observations such as those of refs 5 and 6 are in fact not inconsistent with virtual transfer.

Model with Decay in the Intermediate State

The above simple model is most likely inadequate for describing the primary charge separation. For example, it is possible that E is very small for at least some of the vibrational levels participating in the reaction, so that $E \ll V$; this would help explain the fast rate ($\sim 10^{12}$ s^{-1}, see, e.g., ref 1). If we try to obtain a very fast rate by decreasing the energy denominator, we eventually enter a regime in which the rate constant is not well defined. In the extreme case where $E = 0$ (or more generally $E \ll V \ll \hbar\Gamma$), the population of state 1 oscillates[17] with magnitude 1 at the frequency $V/\hbar$ while the magnitude slowly decays at the rate $2V^2/\hbar^2\Gamma$ (supposing $V_{12} = V_{23} = V$). The population of the intermediate state would get close to 1 in this case. This type of behavior is clearly in conflict with the observed absorption kinetics. To have a well-defined rate constant, we introduce decay in the intermediate state, representative of vibrational dynamics and dephasing processes that depopulate or destroy the phase coherence of the intermediate state vibrational level. Call this decay Γ_2 and from now on refer to the decay in state 3 as Γ_3. Because of this decay, the intermediate state develops an energy width $\hbar\Gamma_2$ that effectively replaces E when E becomes smaller than this width; more generally $E \rightarrow E - i\hbar\Gamma_2$. The dephasing also introduces the possibility of two-step transfer, which was not present in the above model. Note that in this model, there is no pure dephasing; all dephasing in the intermediate state is accompanied by population decay out of the intermediate via Γ_2, so we can keep track of how much population loses coherence in state 2 by calculating the population dropping out of state 2.

We now set $E = 0$ (which certainly falls into the regime $E \ll V$) and examine the behavior of the system when $V \ll \hbar\Gamma_2, \hbar\Gamma_3$. The situation is illustrated in Figure 1b. It is shown in the Appendix that the virtual rate is

$$k_{13} \simeq 2\left(\frac{V_{12}V_{23}}{\hbar\Gamma_2}\right)^2 \frac{1}{\hbar^2\Gamma_3} \qquad (5)$$

Comparing with eq 3, we see that the "effective energy denominator" is just $\hbar\Gamma_2$, as expected.

We now wish to estimate the population on state 2, still in this regime. We can use the same expression stated earlier with the replacement $E \rightarrow -i\hbar\Gamma_2$. The maximum virtual contribution to the population in state 2 is then

$$P_{2MAX} \sim 4(V_{12}/\hbar\Gamma_2)^2 \qquad (6)$$

which by hypothesis is small compared to 1. Just how small this is depends on the identification of the parameters of this simple model with more realistic descriptions of the system.

We would like to identify the parameters appearing in this discussion with parameters of the more complete description in terms of vibrational energy surfaces for the purposes of making population estimates. The matrix elements appearing in this simple model represent the actual electronic matrix elements that one might calculate from molecular orbitals multiplied by vibrational Franck–Condon factors between the dominant vibrational levels. The values of the matrix elements are at present highly uncertain; for want of a better estimate we take $V_{12} \sim 20$ cm^{-1}.[18] Now we identify the decay rates Γ_2 and Γ_3. In the semiclassical regime[19-23] one factor that limits the amount of mixing into the intermediate state is the time for the vibronic force to significantly lower the overlap between the initial state and a transferred wavepacket. This is the "Franck–Condon" time, $\tau_{FC} = \hbar(\lambda\hbar\omega \coth(\hbar\omega/2k_BT))^{-1/2}$. Here λ typifies the reorganization energies of each of the transitions, ω is a typical frequency of a vibrational mode coupled to the transitions, and T is the temperature. Broadening of level 2 may arise from damping or pure dephasing, which are characterized by the coherence time in state 2, τ_{COH_2}. When the coherence time is short compared to a typical vibrational period, so a transferred wavepacket never returns to the crossing surface coherently, the time playing the role of $1/\Gamma_2$ is the shorter of the two times τ_{FC} and τ_{COH_2}; likewise for $1/\Gamma_3$. This is because coherent mixing ceases after one of these times has elapsed.

To obtain an order of magnitude estimate, we assume τ_{FC} is the shorter time scale. Taking $\lambda \sim 600$ cm^{-1} (roughly half the reorganization energy associated with the overall electron transfer[24]), $\hbar\omega \sim 200$ cm^{-1}, and $T \sim 300$ K then gives $\Gamma_2 \sim 500$ cm^{-1}. This yields an estimated $P_{2MAX} \sim 1\%$. While this seems small, it must be remembered that state 1 in this model is just one of the vibrational levels in the initial electronic state, and similarly for states 2 and 3 in the intermediate and final electronic states, respectively. If a few other levels contribute to the intermediate state population, the population could achieve several percent, which could be large enough to understand the Holzapfel absorption kinetics data. This is considering purely the contribution to the intermediate state population due to virtual transfer. It is also possible that the reaction is not in the semiclassical limit and that the coherence time is long compared to a typical vibrational period, in which case it seems reasonable to identify $1/\Gamma_2$ with τ_{COH_2}, since then dephasing limits the extent of coherent mixing.

This model also contains a two-step process, because the inclusion of decay in state 2 leads to a well-defined rate k_{12} in addition to the well-defined rate k_{23}. One may imagine another state, called 2', that receives all the population decaying out of state 2. This may symbolize all the other vibrational levels in the intermediate electronic state. Similarly, we can imagine a state 3' collecting the population decaying out of state 3. The simple model including the symbolic states 2' and 3' is depicted in Figure

(17) Reimers, J. R.; Hush, N. S. *Chem. Phys.* **1989**, *134*, 323.

(18) Warshel, A.; Creighton, S.; Parson, W. W. *J. Phys. Chem.* **1988**, *92*, 2696.
(19) Hopfield, J. J. *Proc. Natl. Acad. Sci. U.S.A.* **1974**, *71*, 3640.
(20) Onuchic, J. N.; Wolynes, P. G. *J. Phys. Chem.* **1988**, *92*, 6495.
(21) Bialek, W.; Bruno, W. J.; Joseph, J. S.; Onuchic, J. N. *Photosynth. Res.* **1989**, *22*, 15.
(22) Onuchic, J. N.; Goldstein, R. F.; Bialek, W. In *Perspectives in Photosynthesis*; Jortner, J., Pullman, B., Eds.; D. Reidel Publishing Co.: Dordrecht, Holland, 1990.
(23) Joseph, J. S.; Bialek, W., to be published.
(24) Woodbury, N.; Parson, W. W. *Biochim. Biophys. Acta* **1984**, *767*, 345.

1c. Population appears in state 2′ at the rate k_{12}, from which it may proceed on to state 3′ via the rate k_{23}. In an experiment on the actual system, one measures the total population in electronic state 2, which corresponds to the sum of the populations in our states 2 and 2′. The population in state 2′ is just the familiar two-step expression, and is never close to 1 if $k_{23} \gg k_{12}$.

It should be noted that in this perturbative regime with small energy denominator E the rate $k_{12} = 2(V_{12}/\hbar)^2/\Gamma_2$ dominates over the virtual rate k_{13} of eq 5. If instead we are in a regime where k_{12} is not well-defined (say $\Gamma_2 \ll V_{12}$) or where it is thermally suppressed (as in an uphill reaction), the virtual rate can be dominant while being perturbative. Whether the observed magnitude of the rate can be understood within that regime, however, depends on the size of the electronic matrix elements and other parameters that remain somewhat uncertain.

It is not yet clear whether k_{12} and k_{23} are well-defined in the actual photosynthetic system, nor is it clear whether k_{23} can really be as fast as required by the observed level of bleaching if one interprets the data in terms of a two-step process. We are simply pointing out that making the model more realistic by including decay out of state 2 and making the energy denominator small still results in a contribution to the population of state 2 from virtual transfer.

Strongly Coherent Regime

We can get very fast nearly exponential decay out of state 1 by choosing $\hbar\Gamma_2$, $\hbar\Gamma_3 \sim V_{12}$, V_{23}, so that nondegenerate perturbation theory breaks down. This may occur if the vibrational dynamics are sufficiently quantum mechanical and if the coherence times are somehow long enough. We now show that in this regime the observable population in state 2 may be dominated by the contribution from virtual transfer, even though two-step processes may make a significant contribution to the overall rate. This is exactly the opposite of what one might have expected—in this limit the intermediate state population is in a sense diagnostic of the virtual and not the two-step process.

To understand the behavior in this regime, first consider two degenerate states coupled by a matrix element V (assumed real and positive) with decay Γ_2 in state 2. As we lower Γ_2 so that its order of magnitude approaches $V/\hbar$, the decay of the state 1 amplitude speeds up and starts to become noticeably biexponential. In the extreme case $\hbar\Gamma_2 = 2V$, the state 1 population evolves as $P_1(t) = [(1 + Vt/\hbar)e^{-Vt/\hbar}]^2$. This curve approximates a single exponential. We say, speaking somewhat loosely, that the rate is $k = 2V/\hbar$, the Rabi rate. [Note that the transition to this "Rabi limit", with the associated breakdown of the Golden Rule, has nothing to do with the transition to adiabaticity à la Landau and Zener.] Decreasing Γ_2 further introduces oscillating components into the state 1 population.

The simplest way this regime might pertain to the primary separation is within a two-step picture. The first step could be a usual Golden Rule rate proportional to V_{12}^2, while the second step has a Rabi rate of order $2V_{23}/\hbar$ (although this almost certainly competes with vibrational relaxation in electronic state 2, about which more will be said later). Another possibility, however, is the three-state analogue of this highly coherent regime, in which a significant fraction of the population passes through the intermediate state without losing phase coherence.

To investigate this strongly coherent regime, consider the three states to be degenerate. Motivated by ref 25, we try $V_{23} = 6V_{12}$ and also use $\hbar\Gamma_2 = 2V_{12}$ and $\hbar\Gamma_3 = 12V_{12}$. [We also notice that a small Γ_2 makes the level very sharp and would thus be expected to make the rate resonantly dependent on the electronic energy gaps, in apparent contradiction to Stark effect absorption kinetics data.[26] It is not yet clear whether a more complete description of the system could avoid this feature.] The resulting peak population in state 2 is less than 4%. This however does not include

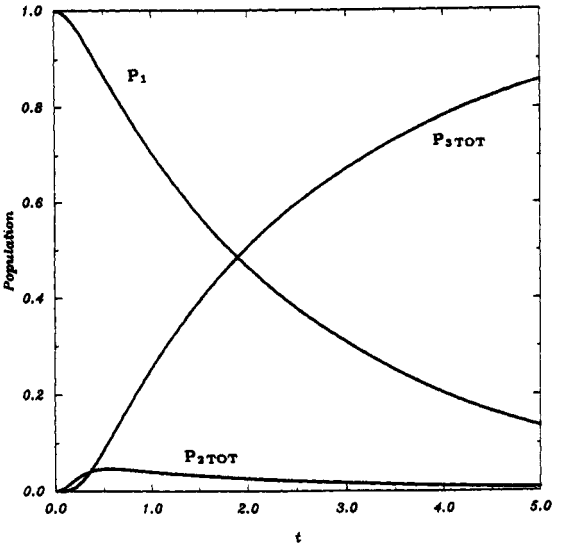

Figure 2. Total populations on electronic states 1, 2, and 3 as functions of time in a regime with long coherence times. The parameters are $V_{23} = 6V_{12}$, $\Gamma_2 = 2V_{12}/\hbar$, $\Gamma_3 = 12V_{12}/\hbar$, $E = 0$. Time is in units of $\hbar/V_{12}$. A rate $k_{23} = 2V_{23}/\hbar$ from state 2′ to state 3′ (two-step process) is included. The total populations on states 2 and 3 are defined as $P_{2TOT} \equiv P_2 + P_{2'}$ and $P_{3TOT} \equiv P_3 + P_{3'}$. The peak total population on the intermediate electronic state due to both virtual and two-step processes is about 0.05, which is small enough to be consistent with the data on bleaching of the monomer band.

the population that decays out of state 2 via Γ_2 into the fictitious state 2′. A measurement of the bleaching reveals the total population of the electronic state 2 (P^+B^-), which is the sum of P_2 and the two-step contribution $P_{2'}$. We may crudely estimate this two-step contribution by including a rate $k_{23} = 2V_{23}/\hbar$ out of state 2′ into state 3′. This results in the plots of Figure 2, showing $P_1(t)$, the total population $P_{2TOT}(t) \equiv P_2(t) + P_{2'}(t)$ in electronic state 2, and the total population $P_{3TOT}(t) \equiv P_3(t) + P_{3'}(t)$ in electronic state 3. We know $P_{2'MAX} \leq (\hbar\Gamma_2/V_{23})P_{2MAX} < 0.02$, since we find the maximum by setting $d/dt\, P_{2'}(t) = 2\Gamma_2 P_2(t) - k_{23}P_{2'}(t) = 0$. Thus, the total population in P^+B^- is not expected to exceed 6% with these parameters, and from the plot the peak is seen to be actually less than 5%. The precise value of the peak population varies considerably with the matrix elements and dephasing rates. The example here demonstrates that a high degree of coherence can help achieve a fast rate but does not necessarily lead to a large accumulation of population in the intermediate state. It is interesting to note that here most of the peak population in the intermediate electronic state is due to the *virtual* process (~4%) and not two-step (<2%) as is usually thought to be the case. Note also that the decay of state 1 approximates a single exponential with a decay rate on the order of $V_{12}/\hbar$, so the final state population $P_3 + P_{3'}$ rises approximately as the corresponding single-exponential growth (since the intermediate state population is always much smaller than 1), and we have fast transfer with a single time constant.

Does this regime correspond to virtual or two-step transfer? The defining characteristic of virtual transfer is that the phase of the state vector is not randomized while the system passes through the intermediate state. In our simple model, that corresponds to passing through 2 without dropping into 2′ (our model includes no pure dephasing). One can estimate how much population drops into 2′ (ignoring k_{23}, which does not change this) as

$$P_{2'TOTAL} = 2\Gamma_2 \int_0^\infty dt\, P_2(t) \sim 2\Gamma_2 \tau P_{2MAX} \sim 0.5 \quad (7)$$

where the time constant τ has been taken from a plot of $P_2(t)$ (not shown) as approximately $\tau \simeq 3\hbar/V_{12}$. The remaining 0.5 of the total system population passes through state 2 coherently. It therefore seems appropriate to say that both virtual and two-step transfer make comparable contributions with these parameters.

(25) Plato, M.; Mobius, K.; Michel-Beyerle, M. E.; Bixon, M.; Jortner, J. *J. Am. Chem. Soc.* **1988**, *110*, 7279.
(26) Lockhart, D. J.; Kirmaier, C.; Holten, D.; Boxer, S. G. *J. Phys. Chem.* **1990**, *94*, 6987.

TABLE I: Summary of Different Regimes

regime	peak total population of intermediate states	comments
$V_{12}, V_{23} \ll E, \hbar\Gamma_3$; $\Gamma_2 = 0$	$4(V_{12}/E)^2$ ($\lesssim$10%)	no two-step process
$V_{12}, V_{23} \ll \hbar\Gamma_3$; $E = \hbar\Gamma_2 = 0$	~100%	oscillatory populations no two-step process
$V_{12}, V_{23} \ll \hbar\Gamma_2, \hbar\Gamma_3$; $E = 0$	$<4(V_{12}/\hbar\Gamma_2)^2 + x^{1/(1-x)}$	two-step transfer dominant[a]
$V_{23} = 6V_{12}$; $\hbar\Gamma_2 = 2V_{12}$; $\hbar\Gamma_3 = 12V_{12}$; $E = 0$	5%	transfer is roughly half two-step and half virtual

[a] Here $x \equiv k_{12}/k_{23} = [V_{12}^2/(\hbar^2\Gamma_2)]/[V_{23}^2/(\hbar\Gamma_3)]$. This term represents the peak due to the two-step process, and could a priori be anywhere from 0 to 100%. The first term is due to the virtual process and is $\ll$100% by hypothesis in that regime. The combined expression in the table is an upper bound, since the peaks of the two processes generally do not occur simultaneously.

Summary and Discussion

We have shown within the context of a simple three-state model that the process of virtual transfer makes a contribution to the population of the intermediate state as measured by absorption bleaching in the B band. The maximum attained by this contribution during the course of the charge separation could be close to 1 or it could be less than 10^{-2}, depending on the parameters. Some plausible parameters result in 5–10% bleaching, which is comparable to the effect seen by Holzapfel et al.,[5,6] while it also plausible to have a much smaller effect than that, as seen by Kirmaier and Holten.[7] The observation of a near absence of bleaching in the B band certainly rules out those regimes in which it gets close to 1. However, the observation of some small but nonzero bleaching would not necessarily rule out the mechanism of virtual transfer. In fact, it is possible that most of the observed bleaching is due to virtual transfer and not a two-step process. Furthermore, the question of which process dominates the bleaching is largely independent of which process dominates the transfer, as seen by our last example.

The main features of the various regimes considered are summarized in Table I, in which we recapitulate the peak total population of the intermediate due to all processes, since that is what is seen in experiments.

The absorption measurements do eliminate some regimes but do not rule out all schemes involving virtual transfer. We might hope to identify virtual transfer experimentally by linear growth in the population of the final state during an intermediate range of times, but a two-step process could have the same appearance if $k_{12} \ll k_{23}$. Besides, the strongly coherent regime discussed in the last section displayed a final state population that was only approximately single exponential, yet virtual transfer plays a significant role there. Using shorter pulses might not lift the ambiguity, since the short-time behavior in any case is complicated and depends on the details of the vibrational coupling.

If vibrational cooling in the intermediate state occurs on a time scale comparable to the second transition, we cannot expect exponential kinetics in a two-step process even at "long" times. Even if the first transition is well described by a rate constant, the second transition might be so fast as to compete with vibrational equilibration in the intermediate state, leading to a second step that is nonexponential and a final state population that is not really composed of simple exponentials. An interesting feature of the analysis of Holzapfel et al.[5,6] is that the second rate of their fitted two-step process, 0.9 ps, is so fast that it might compete with equilibration in P^+B^-. This suggests that it may not be consistent to assign this observed "rate" to a simple chemical kinetic step. One might still see single-exponential growth on the final state if the (nonexponential) second step is fast enough. Assuming that a fit with two exponentials does give a significantly better fit than a fit with only one, it is not yet clear what functional form would be appropriate for the second step if we believe it is indeed nonexponential. Neither does the superiority of a two-exponential fit necessarily imply a predominantly two-step transfer.

While absorption kinetics measurements do have the power of ruling out certain schemes for the primary transfer mechanism, it appears that other types of data will be needed to determine the mechanism completely.

Acknowledgment. We have benefitted from conversations with W. Gerstner and S. Franzen. This work was funded in part by the Regents of the University of California (J.S.J.), a Department of Education fellowship (W.B.), and a National Science Foundation Presidential Young Investigator Award (W.B.), supplemented by funds from Cray Research Inc., Sun Microsystems, and the NEC Research Institute.

Appendix

Here we calculate the virtual rate in the regime $E = 0$ and $V_{12}, V_{23} \ll \hbar\Gamma_2, \hbar\Gamma_3$. Merely looking at the rate of decay of state 1 can be deceptive, since that rate is $k_{12} + k_{13}$ in the presence of both two-step and virtual processes. While k_{13} is proportional to $V_{12}^2V_{23}^2$ at lowest order in perturbation theory, the rate constant k_{12} also has a contribution in perturbation theory of order $V_{12}^2V_{23}^2$. Therefore, calculating the decay rate of state 1 at order $V_{12}^2V_{23}^2$ will not tell us the virtual rate k_{13}. Instead, we imagine a state 3′ which receives all the population that decays from state 3 via Γ_3, so that

$$\frac{d}{dt} P_{3'}(t) = 2\Gamma_3 P_3(t) \tag{8}$$

State 3′ might be thought of as representing the lower vibrational levels of electronic state 3 in the actual system. Analogously, we may introduce a state 2′ representing the other levels of the intermediate electronic state. The simple model including the states 2′ and 3′ is depicted in Figure 1c. The population of state 3′ should grow linearly with time with slope k_{13} for times much shorter than $1/k_{12}$ but much longer than $1/\Gamma_2$ and $1/\Gamma_3$. It is necessary for the time to be short compared to $1/k_{12}$ to see linear growth, because the rate of growth due to the virtual process is $k_{13}P_1(t)$, and $P_1 \simeq 1$ only for such short times. For such intermediate times, $d/dt\ P_{3'}(t) \simeq$ constant, and we may identify this constant with the virtual rate k_{13}. (Note that the two-step process contribution to the state 3′ population does not appear here; we discuss this contribution in the main text.)

Inserting an approximate expression for $P_3(t)$ gives

$$\frac{d}{dt} P_{3'}(t) \simeq 2\Gamma_3 V_{12}^2 V_{23}^2 \left| \frac{1}{\hbar^2\Gamma_2\Gamma_3} \exp\{-tV_{12}^2/(\hbar^2\Gamma_2)\} + \frac{1}{\hbar^2\Gamma_2(\Gamma_2 - \Gamma_3)} \exp\{-t\Gamma_2\} - \frac{1}{\hbar^2\Gamma_3(\Gamma_2 - \Gamma_3)} \exp\{-t\Gamma_3\} \right|^2 \tag{9}$$

[The validity of this approximate expression for $P_3(t)$ requires, in addition to $V_{12}, V_{23} \ll \hbar\Gamma_2, \hbar\Gamma_3$, that Γ_2 does not precisely equal Γ_3. The amplitudes of the exponentials $e^{-t\Gamma_2}$ and $e^{-t\Gamma_3}$ must not be significant at the intermediate times of interest. Considering times of order $\hbar/|V_{12}|$, we therefore require $[1/|\Gamma_2 - \Gamma_3|] \exp(-\hbar\Gamma_2/|V_{12}|) \ll 1/\Gamma_3$ and also $[1/|\Gamma_2 - \Gamma_3|] \exp(-\hbar\Gamma_3/|V_{12}|) \ll 1/\Gamma_2$. The exponentially small factors makes these conditions easy to satisfy.]

We have not included in this expression the proper oscillatory phase factors for the three terms, because for the intermediate times of interest only the first term is significant and the remaining phase factor has no effect on the population. It can be seen that for times such that $\Gamma_2 t \gg 1$ and $\Gamma_3 t \gg 1$ and $V_{12}^2/(\hbar^2\Gamma_2)t \ll 1$ the population of 3 is essentially constant and the population of 3′ grows linearly. We then identify the virtual rate as

$$k_{13} \simeq 2\left(\frac{V_{12}V_{23}}{\hbar\Gamma_2}\right)^2 \frac{1}{\hbar^2\Gamma_3} \tag{10}$$

This has precisely the same form as the virtual rate in the situation with $E \gg V$ and $\Gamma_2 = 0$, except that E has been replaced by $\hbar\Gamma_2$. This shows that it is $\hbar\Gamma_2$ and not V that determines when E is

too small for the usual virtual rate expression $k_{13} = 2(V_{12}V_{23}/E)^2/\hbar^2\Gamma_3$ to hold. It also shows that nondegenerate perturbation theory is still valid even when $E \ll V$, because then dephasing processes in state 2 change the validity criterion to $V \ll \hbar\Gamma_2$. Reimers and Hush[17] did not consider any form of dephasing or vibrational dynamics in state 2 and so were led to a rate that became nonperturbative and strongly E-dependent when $E \ll V$. It is shown in the main text that the effective width $\hbar\Gamma_2$ could be much larger than the matrix elements, in which case the virtual rate is still perturbative, varies with E only gradually on the energy scale $\hbar\Gamma_2$, and is not nearly as fast as it would be if Γ_2 were zero. The inclusion of Γ_2 also leads to a state 1 population that eventually becomes a decaying exponential rather than an exponentially decaying oscillation.

CIDEP Study of the Photoreduction of Xanthone in Alcohols: Novel Indirect Hydrogen Abstraction Steps

Hisao Murai and Keiji Kuwata*

Department of Chemistry, Faculty of Science, Osaka University, Toyonaka, Osaka 560, Japan
(Received: December 4, 1990; In Final Form: January 30, 1991)

The photoreduction of xanthone in ethanol and deuterated ethanol (C_2H_5OD) was studied by using time-resolved ESR spectroscopy. The CIDEP spectra assigned to the alcohol radical and the xanthone ketyl radical show an E/A* pattern, in place of the ordinary emissive TM spin polarization by the photoexcited xanthone. At the hydroxyl group of the ketyl radical formed in C_2H_5OD has a deuterium, which is abstracted from the OD group of C_2H_5OD by xanthone in the triplet state. An indirect hydrogen abstraction process such as a charge transfer followed by a proton transfer is postulated.

The photochemistry of aromatic ketones such as benzophenone in alcoholic solution is known to be a direct hydrogen abstraction from alcohols to form the ketyl radicals and the alcohol radicals (hydroxyalkyl radicals).[1] The most reactive site of primary and secondary alcohols as reductants is usually the CH or CH_2 group where the hydroxyl group is attached. In the system of photoexcited *p*-quinones in alcohols, however, the formation of the alkoxy radicals as the reaction intermediates has been reported.[2] In this article, the evidence of a novel hydrogen abstraction from the hydroxyl group of alcohol by the photoexcited xanthone is presented.

Xanthone is one of the aromatic ketones that shows hydrogen abstraction in alcoholic media as well.[3] Xanthone is known to have $\pi\pi^*$ orbital character as the lowest excited triplet state in low-temperature matrices[4] and also in polar solvents.[3] The higher $n\pi^*$ triplet state is located close to the $\pi\pi^*$ one, and the separation is sensitively affected by the environment. These properties of xanthone show the dual phosphorescence phenomenon.[5] Xanthone is also known to show unusual hydrogen abstraction to form the cyclohexadienyl-type radicals when special reductants such as triethylgermanium hydride and sodium borohydride are employed.[6]

The photoreduction of xanthone in ethanol (C_2H_5OH) and partially deuterated ethanol (C_2H_5OD), 99.5+ atom % D) was carefully studied by using an X-band time-resolved ESR (trESR) technique at near 0 °C. As the pulsed light source, a XeF excimer laser (Lumonics EX-510, λ = 351 nm) was used. The concentration of xanthone was 1×10^{-2} mol dm^{-3}, and the solution was deoxygenated by bubbling with pure nitrogen gas prior to the trESR measurements.[7]

In Figure 1a, the solid line shows the α-hydroxyethyl radical (ethanol – H radical) having an emissive/absorptive* (E/A*; the asterisk denotes an absorptive deviation) pattern and the xanthone ketyl radical also having an apparent E/A*. These E/A* patterns are thought to be due to the superposition of an E/A by radical pair mechanism (RPM) and an enhanced absorption by triplet mechanism (TM) of chemically induced dynamic electron polarization (CIDEP).[8] The ethanol – H radical, which has the structure of hydrogen abstracted at the methylene group, and the xanthone ketyl – H radical are satisfactorily simulated as shown by the solid-line spectrum in Figure 1b by using hfc constants reported previously.[9,10] The hfc constants of the hydroxyl protons of the xanthone ketyl – H radical and the ethanol – H radical used in this simulation are 0.250 and 0.050 mT, respectively. This result seems to be explained by the ordinary direct hydrogen abstraction reaction, but the absorptive TM polarization components observed in this particular system are very mysterious, while photoexcited xanthone is known to show emissive TM polarization.[6,7a] Similar absorptive polarization was observed in the other alcohols such as 2-propanol and isobutyl alcohol.

When C_2H_5OH was substituted by C_2H_5OD, a quite different trESR spectrum was observed, as shown by broken line in Figure 1a. First, the ketyl – D radical, which has an E/A* pattern, is well simulated by changing the hfc constant of the proton of the OH group to that of deuteron ($I = 1$, $a_{OD} = a_{OH}/6.5$) as shown in Figure 1b by a broken line. This reveals that the deuterium abstraction takes place at the OD group of C_2H_5OD. Second, each hf line of the ethanol radical in the system of C_2H_5OD is much sharper than that in the system of C_2H_5OH. This implies that the alcohol radical has an OD group in the system of C_2H_5OD, contrary to the reactive site of the hydrogen abstraction in the OD group as mentioned above. Therefore, the alkoxyl radical, which is expected to be formed transiently, may react with the other alcohol molecules very quickly.[7a]

(1) (a) Beckett, A.; Porter, G. *Trans. Faraday Soc.* **1963**, *59*, 2038. (b) Cohen, S. G.; Litt, A. D. *Tetrahedron Lett.* **1970**, 837.
(2) McLauchlan, K. A.; Sealy, R. C. *J. Chem. Soc., Chem. Commun.* **1976**, 115.
(3) Scaiano, J. C. *J. Am. Chem. Soc.* **1980**, *102*, 7747.
(4) (a) Murai, H.; Minami, M.; I'Haya, Y. J. *J. Phys. Chem.* **1988**, *92*, 2120. (b) Chakrabarti, A.; Hirota, N. *J. Phys. Chem.* **1976**, *80*, 2966. (c) Griesser, H. J.; Bramley, R. *Chem. Phys.* **1982**, *67*, 373.
(5) (a) Pownall, H. J.; Mantulin, W. W. *Mol. Phys.* **1976**, *31*, 1393. (b) Connors, R. E.; Walsh, P. S. *Chem. Phys. Lett.* **1977**, *52*, 436. (c) Vala, M.; Hurst, J.; Trabjerg, I. *Mol. Phys.* **1981**, *43*, 1219. (d) Connors, R. E.; Christian, W. R. *J. Phys. Chem.* **1982**, *86*, 1524.
(6) (a) Sakaguchi, Y.; Hayashi, H.; Murai, H.; I'Haya, Y. J. *J. Am. Chem. Soc.* **1988**, *110*, 7479. (b) Sakaguchi, Y.; Hayashi, H.; Murai, H.; I'Haya, Y. J.; Mochida, K. *Chem. Phys. Lett.* **1985**, *120*, 401.
(7) (a) Ohara, K.; Murai, H.; Kuwata, K. *Bull. Chem. Soc. Jpn.* **1989**, *62*, 2435. (b) Murai, H.; Kuwata, K. *Chem. Phys. Lett.* **1989**, *164*, 567.
(8) McLauchlan, K. A. *Advanced EPR: Applications in Biology and Biochemistry*; Hoff, A. J., Ed.; Elsevier: New York, 1989; pp 345–369 and references therein.
(9) Livingstone, R.; Zeldes, H. *J. Chem. Phys.* **1966**, *44*, 1245.
(10) Wilson, R. *J. Chem. Soc. B* **1968**, 1581.
(11) Wilson, R. *J. Chem. Soc. B* **1968**, 84.

0022-3654/91/2095-6247$02.50/0